

Chiral Lithium Amide/Solute Complexes: X-ray Crystallographic and NMR Spectroscopic Studies

Göran Hilmersson, Per I. Arvidsson, and Öjvind Davidsson*

Department of Organic Chemistry, Göteborg University, S-412 96 Göteborg, Sweden

Mikael Håkansson

Department of Inorganic Chemistry, Chalmers University of Technology,
S-412 96, Göteborg, Sweden

Received November 22, 1996[⊗]

We have shown by the use of multinuclear and multidimensional NMR that the reaction mixture of [⁶Li]lithium (2-methoxy-(*R*)-1-phenylethyl)((*S*)-1-phenylethyl)amide (**2**) and cyclohexene oxide in DEE results in the formation of monomeric and dimeric complexes between **2** and cyclohexene oxide at $-80\text{ }^{\circ}\text{C}$. The dimeric complex of **2** exhibited a slow cyclohexene oxide substitution rate on the NMR time scale that was found to be controlled by a dissociative mechanism. The ⁶Li,¹H-HOESY NMR spectrum of the above reaction mixture showed NOE's between lithium and cyclohexene oxide protons in both the monomer and dimer complexes of **2**. A single-crystal X-ray diffraction experiment revealed that the solid state structure of **2**, crystallized from THF, is dimeric with a planar Li₂N₂ core constructed from amido nitrogen bridges. Both methoxy groups coordinate terminally to one lithium atom, Li(1), making it four-coordinated, while the other lithium, Li(2), binds to one THF and thus is three-coordinated. The dilithiated amide, [⁶Li]lithium (2-methoxy-(*R*)-1-phenylethyl)(2-(⁶Li)lithio)-(S)-1-phenylethyl)amide (**4**) was obtained by reaction of 1 equiv of [⁶Li]-*n*-BuLi with **2** in DEE at 25 °C for 3–5 h. The lithium amide **4** aggregates, giving a tetrameric lithium core consisting of two molecules of **4**. A titration study of **4** in DEE with THF also showed that **4** exhibited slow ligand substitution rates on the NMR time scale. The dimer **4** exhibited a slow cyclohexene oxide substitution rate that was found to be controlled by an associative mechanism. The lithium amide **2** has been used for the deprotonation and ring opening of cyclohexene oxide, giving an ee of 47% of the (*R*)-cyclohexen-1-ol. The deprotonation of cyclohexene oxide using **4** gave on the other hand the (*S*)-cyclohexen-1-ol with an ee of 41%. The rate of reaction was found to be initially 1.5 times faster using **4** compared to using **2** in DEE. This is probably due to the fact that the deprotonation of cyclohexene oxide is performed by the carbanionic carbon base and not by the lithium amide base in **4**. The lithium salt of (2-methoxy-(*R*)-1-phenylethyl)((*R*)-1-phenyl-2-methylpropyl)amine (**5**) was prepared, as a potential reagent for the deprotonation of cyclohexene oxide, from our NMR studies of lithium amide reagent–substrate complexes. The ee increased in the deprotonation reaction from the previous 47% to 74% in the (*R*)-cyclohexen-1-ol.

Introduction

Chiral lithium amide bases are presently receiving much attention in the field of enantioselective proton transfer reactions, either protonation or deprotonation.¹ Enantioselective deprotonation of several prochiral epoxides has previously been performed utilizing various

chiral lithium amide bases.^{2,3} Deprotonation reactions of epoxides are proposed to proceed through a cyclic six-membered transition state wherein the proton is removed *syn* to the epoxide oxygen (Scheme 1). There are also suggestions that the reacting specie is a monomer, constituted by one epoxide and one lithium amide molecule.⁴

The obtained enantioselectivity in the product utilizing chiral lithium amide bases is suggested to be due to an unfavorable steric interaction in the transition state, see above. Attempts to increase the enantiomeric excess by introduction of bulky substituents, by Bhuniya and co-workers, X in Figure 1, have not been fruitful;

* Phone: +46 31 7722895. Fax: +46 31 7723840. E-mail: Öjvind.Davidsson@oc.chalmers.se.

[⊗] Abstract published in *Advance ACS Abstracts*, June 15, 1997.

(1) (a) Simpkins, N. S. *Chem. Ind.* **1988**, 20, 387. (b) Cain, C. M.; Cousins, R. P. C.; Coumbarides, G.; Simpkins, N. S. *Tetrahedron* **1990**, 46, 523. (c) Ward, R. S. *Chem. Soc. Rev.* **1990**, 19, 1. (d) Cox, P. J.; Persad, A.; Simpkins, N. S. *Synlett* **1992**, 194. (e) Coggins, P.; Simpkins, N. S. *Synlett* **1992**, 313. (f) Underiner, T. L.; Paquette, L. A. *J. Org. Chem.* **1992**, 57, 5438. (g) Honda, T.; Kitamura, N.; Tsubuki, M. *Tetrahedron: Asymmetry* **1993**, 4, 21. (h) Honda, T.; Kitamura, N.; Tsubuki, M. *Tetrahedron: Asymmetry* **1993**, 4, 1475. (i) Sabukawa, M.; Koga, K. *Tetrahedron Lett.* **1993**, 34, 5101. (j) Aoki, K.; Noguchi, H.; Tomioka, K.; Koga, K. *Tetrahedron Lett.* **1993**, 34, 5105. (k) Asami, M.; Ishizaki, T.; Inoune, S. *Tetrahedron: Asymmetry* **1994**, 5, 793, see also refs 2a,b, 3a–d.

(2) (a) Cox, P. J.; Simpkins, N. S. *Tetrahedron: Asymmetry* **1991**, 2, 1. (b) Koga, K. *Pure Appl. Chem.* **1994**, 66, 1487, see also ref 1b.

(3) (a) Asami, M. *Tetrahedron Lett.* **1984**, 26, 5803. (b) Asami, M.; Kirihara, H. *Chemistry Lett.* **1987**, 389. (c) Asami, M. *Chem. Lett.* **1984**, 829. (d) Asami, M. *Bull. Chem. Soc. Jpn.* **1990**, 63, 1402. (e) Bhuniya, D.; DattaGupta, A.; Singh, V. K. *J. Org. Chem.* **1996**, 61, 6108.

(4) Thummel, R. P.; Richborn, B. *J. Am. Chem. Soc.* **1970**, 92, 2064, see also ref 3e.

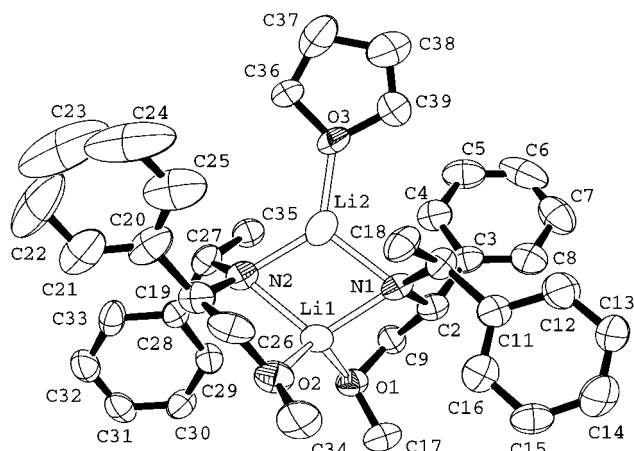
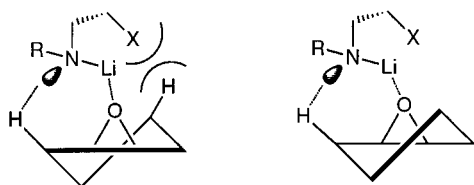


Figure 1. Crystallographic numbering in *(R,S)*-**2**. The planar Li_2N_2 core exhibits lithium atoms with different coordination numbers.

Scheme 1



instead, the ee markedly decreased using these more substituted lithium amides.⁵ This observation could indicate that the proposed transition state (TS) structure is not the correct one. Effects of additives in these reactions, e.g. hexamethylphosphoramide (HMPA), 1,3-dimethyl-3,4,5,6-tetrahydro-2(1*H*)-pyrimidinone (DMPU), and *N,N,N,N*-tetramethylethylenediamine (TMEDA), have been reported to result in more stereoselective reagents; however, their mode of action except for their high propensity of deaggregation is still unclear.

Although several different chiral lithium amide bases have been prepared and used in asymmetric transformations, only a few structure investigations in solution or in the solid state have been reported.⁶ Therefore, it is of great importance to obtain solution and/or solid state structures of these chiral lithium amide bases. These structural investigations give information about possible initial states (IS) which might reflect possible TS structures. A comparison between the two possible *re* and *si* associations of an epoxide to the determined solution or solid state structure of a chiral lithium amide base could give an idea of the stereochemical outcome of the enantioselective deprotonation reaction and also how to recall the enantioselectivity in the reactions.

We herein present results showing the solution and solid state structure of two novel lithium amides and their complexes. The dynamics of these lithium amide solvent–substrate complexes has been studied by NMR spectroscopy. Their induction of asymmetry in the deprotonation reaction of cyclohexene oxide has also been investigated.

Results and Discussion

The treatment of (2-methoxy-*(R)*-1-phenylethyl)((*S*)-1-phenylethyl)amine (**1**) with 1 equivalent *n*-butyllithium in diethyl ether-*d*₁₀ (DEE) results in the formation of DEE solvated lithium (2-methoxy-*(R)*-1-phenylethyl)((*S*)-1-phenylethyl)amide (**2b**)⁷ (Scheme 2).

The solution structure of **2b** in DEE and tetrahydrofuran (THF-*d*₈) has previously been determined by use of homo(¹H,¹H-NOESY) and hetero(⁶Li,¹H-HOESY) nuclear Overhauser effects spectroscopy, and it has been shown by solvent titration with THF, DEE and by comparing integral ratios between solvent and amide that there is only one solvent molecule coordinating to **2b** as shown in Scheme 1. The monomer **2a**, which is the major aggregate in THF, has been found to coordinate two solvent molecules.^{8,9} A single-crystal X-ray diffraction experiment revealed that the solid state structure of **2**, crystallized from THF, is dimeric as indicated in **2b** in Scheme 2. The molecular structure and the crystallographic numbering is given in Figure 1, crystallographic details are listed in Table 1, and selected distances and angles are presented in Table 2. As can be seen from Figure 1, the planar Li_2N_2 core is constructed from amido nitrogen bridges, while both methoxy groups coordinate terminally to the same lithium, Li(1), making it four-coordinated.

Since only one THF molecule is bound to Li(2), this metal center exhibits a trigonal planar coordination figure with angles around Li(2) in the 109–130° range. The coordination geometry around Li(1) is approximately tetrahedral, with angles varying from 88 to 127°. Crystal structures of dimeric lithium amides have been reported earlier,¹⁰ but to our knowledge this is the first complex exhibiting a planar Li_2N_2 core with one three- and one four-coordinated lithium. Earlier reports¹⁰ describe the Li_2N_2 core in terms of alternating short and long Li–N bonds, but due to low crystallographic precision in the determination of these bonds, this

(7) The chiral amine (2-methoxy-*(R)*-1-phenylethyl)((*S*)-1-phenylethyl)amine (**1**) was prepared according to a previously described procedure by Hogeveen and Eleveld (Eleveld, M. B.; Hogeveen, H. *Tetrahedron Lett.* **1984**, *25*, 5187). The diastereomeric ratio *S,R* to *S,S* of **1** was analyzed using ¹H NMR and was found to be more than 99% in *S,R* compared to *S,S*. The use of (*S*)-methylbenzylamine in the synthesis of **1** results in an *S* stereoconfiguration at the methyl-substituted carbon C(10)/C(27). The ¹H and ¹³C NMR spectra of **1** and **4** were assigned using ¹H,¹H-DQCOSEY and ¹³C,¹H-HMQC. ¹H NMR chemical shift of **1** in DEE-*d*₁₀ at 21 °C: (500 MHz; DEE-*d*₁₀) δ_H 1.24 (3H, d, *J*₁₂ 6.8, CH₃), 2.30 (1H, s, br, N-H), 3.20 (3H, s, OCH₃), 3.20 (1H, dd, *J*₁₂ 9.4, 3.7, C(9)H), 3.29 (1H, dd, *J*₁₂ 9.3, 9.3, C(9)H), 3.48 (1H, q, *J*₁₂ 6.8, C(10)H), 3.61 (1H, dd, *J*₁₂ 9.4, 3.7, C(2)H), 7.13–7.27 (10H, aromatic protons). ¹³C chemical shift of **1** in benzene-*d*₆ at 21 °C: (125 MHz; benzene-*d*₆) δ_H 25.6 (q, CH₃), 55.5 (d, C(2)), 58.7 (q, OCH₃), 60.1 (d, C(10)), 78.6 (t, C(9)), aromatic carbons, 127.2, 127.3, 127.9, 128.6, 129.0, 129.1, quaternary carbons, 142.2, 146.6. ¹H NMR chemical shift of **4** in DEE-*d*₁₀ at –80 °C: (500 MHz; DEE-*d*₁₀; –80 °C) δ_H 0.98 (3H, d, *J*₁₂ 6.54, CH₃), 2.18 (3H, s, OCH₃), 3.35 (1H, d, *J*₁₂ 7.80, C(9)H), 3.80 (1H, dd, *J*₁₂ 7.85, 3.2, C(2)H), 3.98 (1H, s, C(9)H), 4.54 (1H, q, *J*₁₂ 6.54, C(10)H), 6.86 (1H, t, *J*₁₂ 6.86, C(14)H), 7.05 (1H, d, *J*₁₂ 7.74, C(12)H), 7.16 (1H, t, *J*₁₂ 7.20, C(6)H), 7.17 (1H, t, *J*₁₂ 7.21, C(13)H), 7.31 (2H, t, *J*₁₂ 7.29, C(5)H, C(7)H), 7.62 (2H, s, br, C(4)H, C(8)H), 7.91 (1H, d, *J*₁₂ 6.74, C(15)H).

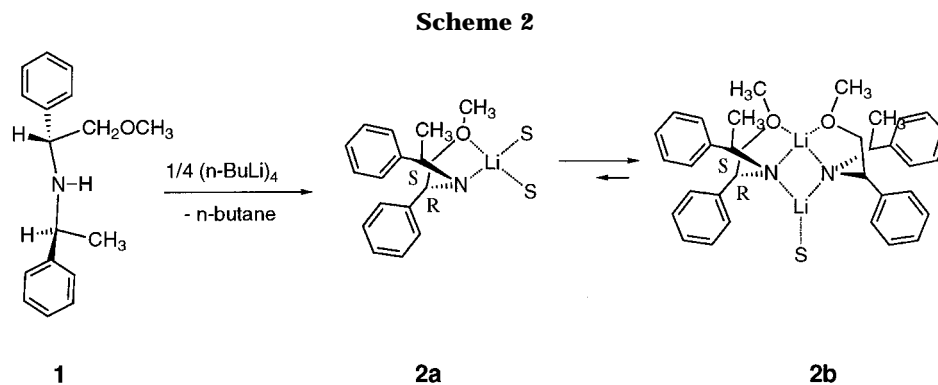
(8) Hilmersson, G.; Davidsson, Ö. *J. Organomet. Chem.* **1994**, *489*, 175.

(9) Hilmersson, G.; Davidsson, Ö. *J. Org. Chem.* **1995**, *60*, 7660.

(10) Setzer, W.; Schleyer, P. v. R. *Adv. Inorg. Chem.* **1985**, *24*, 353. Mulvey, R. E. *Chem. Soc. Rev.* **1991**, *20*, 167. Gregory, K.; Schleyer, P. v. R.; Snaith, R. *Adv. Inorg. Chem.* **1991**, *37*, 47. Barr, D.; Berrisford, D. J.; Jones, R. V. H.; Slawin, A. M. Z.; Snaith, R.; Stoddart, J. F.; Williams, D. J. *Angew. Chem., Int. Ed. Engl.* **1989**, *28*, 1044. Lappert, M. F.; Slade, M. J.; Singh, A.; Atwood, J. L.; Rogers, R. D.; Shakir, R. *J. Am. Chem. Soc.* **1983**, *105*, 302. Barr, D.; Clegg, W.; Mulvey, R. E.; Snaith, R. *J. Chem. Commun.* **1984**, 285. Williard, P.; Salvino, J. M. *J. Org. Chem.* **1993**, *58*, 1.

(5) Bhuniya, D.; Singh, V. K. *Synth. Commun.* **1994**, *24*, 375.

(6) Barr, D.; Berrisford, D. J.; Jones, R. V. H.; Slawin, A. M. Z.; Snaith, R.; Stoddart, J. F.; Williams, D. J. *Angew. Chem., Int. Ed. Engl.* **1989**, *28*, 1044. Sato, D.; Kawasaki, H.; Shimada, I.; Arata, Y.; Okamura, K.; Date, T.; Koga, K. *J. Am. Chem. Soc.* **1992**, *114*, 762.

**Table 1. Crystallographic Data for 2 and 6**

	2	6
formula	C ₃₈ H ₄₈ Li ₂ N ₂ O ₃	C ₃₈ H ₅₂ Cl ₂ N ₂ O ₂
fw	594.7	639.7
cryst syst	orthorhombic	triclinic
space group	<i>P</i> 2 ₁ 2 ₁ 2 ₁ (No. 19)	<i>P</i> 1̄ (No. 2)
<i>a</i> , Å	11.111(5)	9.697(2)
<i>b</i> , Å	32.257(6)	7.3427(13)
<i>c</i> , Å	9.814(4)	13.162(2)
α , deg	90	90.03(2)
β , deg	90	102.78(1)
γ , deg	90	90.01(1)
<i>V</i> , Å ³	3518(2)	913.9(3)
<i>Z</i>	4	1
<i>d</i> _{calc} , g/cm ³	1.123	1.162
<i>F</i> (000)	1280	344
cryst dimens, mm	0.25 × 0.20 × 0.20	0.20 × 0.20 × 0.20
radiation	Mo K α (0.710 73 Å)	Mo K α (0.710 73 Å)
μ , mm ⁻¹	0.069	0.211
<i>T</i> , °C	-120	20
data collected, deg	5.0 < 2 θ < 50.0	5.0 < 2 θ < 50.0
index ranges	+ <i>h</i> ,+ <i>k</i> ,+ <i>l</i>	+ <i>h</i> ,± <i>k</i> ,± <i>l</i>
abs corr	ψ -scans	ψ -scans
transm coeff	0.95–1.00	0.96–1.00
total no. reflns	3224	3445
no. of unique reflns	3224	3445
no. of params refined	406	397
final <i>R</i> indices	<i>R</i> 1 = 0.044, w <i>R</i> 2 = 0.112	<i>R</i> 1 = 0.065, w <i>R</i> 2 = 0.182
max. residual electron density, e/Å ³	0.18	0.65
min. residual electron density, e/Å ³	-0.19	-0.65

Table 2. Selected Intramolecular Distances (Å) and Angles (deg) for 2

Li(1)–O(2)	1.92(2)	Li(1)–O(1)	1.95(2)
Li(1)–N(1)	2.04(2)	Li(1)–N(2)	2.10(2)
Li(1)–Li(2)	2.43(3)	Li(2)–O(3)	1.94(2)
Li(2)–N(2)	1.98(2)	Li(2)–N(1)	2.06(2)
N(1)–C(2)	1.432(11)	N(1)–C(10)	1.463(12)
N(2)–C(19)	1.450(12)	N(2)–C(27)	1.487(12)
Li(1)–N(1)–Li(2)	72.6(8)	Li(2)–N(2)–Li(1)	72.9(8)
N(2)–Li(2)–Li(1)	55.8(7)	N(1)–Li(2)–Li(1)	53.3(6)
N(1)–Li(1)–N(2)	105.4(8)	O(2)–Li(1)–O(1)	124.3(9)
O(2)–Li(1)–N(1)	124.8(9)	O(1)–Li(1)–N(1)	89.3(7)
O(2)–Li(1)–N(2)	88.0(7)	O(1)–Li(1)–N(2)	127.3(9)
O(3)–Li(2)–N(2)	129.8(10)	O(3)–Li(2)–N(1)	120.9(10)
N(2)–Li(2)–N(1)	109.1(10)		

description is questionable. For the same reason it is difficult to rationalize the Li–N distances (or the Li–O distances) in terms of the coordination number of the metal. The hydrogens on C(35) and C(18) are situated around 2.3 Å away from the coordinatively unsaturated Li(2), which consequently is approaching a trigonal bipyramidal coordination geometry.

A heterodimer (**3**) is formed between one molecule *n*-butyllithium and **2a** if 2 equiv of *n*-butyllithium/**1** is used (Scheme 3).¹¹ If **3**, in DEE, is kept at room temperature for some 3–5 h, then an *ortho* proton,

namely the one on the phenyl ring attached to the C(10) carbon, is regioselectively abstracted intramolecularly by the complexed *n*-butyllithium. This regioselectively lithiation reaction proceeds without the need for any addition of lithium coordinating agents such as, for example, TMEDA, Scheme 3. The intramolecular dilithiation of **2b** is tentatively proposed to proceed through the mixed dimer **3**. The ⁶Li NMR spectrum of the resulting dilithiated species, lithium (2-methoxy-(*R*)-1-phenylethyl)(2-lithio-(*S*)-1-phenylethyl)amide (**4**), at -70 °C in DEE revealed two signals at δ 3.04 and 3.16, respectively, of almost identical intensities with the signal at δ 3.04 significantly broader due to lithium–proton coupling. The ¹³C NMR spectrum of **4** showed only one set of carbon signals at all temperatures from +20 to -80 °C, indicative of the presence of only one lithium amide complex in DEE solution.

A ⁶Li NMR temperature dependent study showed that there is an intramolecular lithium exchange in **4** and above -15 °C only one lithium signal is seen from **4** in the ⁶Li NMR spectra.

The ⁶Li,⁶Li-EXSY of **4** also established that the two lithium signals at δ 3.04 and 3.16 exchanged with each other. From the dynamic temperature study of **4** we could estimate a free energy of activation $\Delta G^{\ddagger} \approx 51$ kJ/mol⁻¹ for the lithium–lithium exchange. The temperature dependence of the two lithium-6 signals from **4** showed large similarities with the previously observed temperature dependence for **2b** with only a slightly higher activation energy of entropy for the lithium–lithium exchange in **4** compared to **2b**. The entropy of activation suggests that the reorientation or lithium exchange of the dimer proceeds through an activated complex without association or deassociation of solvent molecules in the TS compared to the IS. The two lithium signals at δ 3.04 and 3.16 in the ⁶Li NMR spectrum were established to have a scalar coupling of ~0.1–0.15 Hz from a ⁶Li,⁶Li-INADEQUATE experiment (Figure 2). This observation unambiguously shows that these two lithiums are present in the same aggregate.

We were not able to resolve any ¹³C–⁶Li couplings in the ¹³C{¹H} NMR spectrum, which would give information about the aggregation state. This is probably due to the different magnitude in coupling constants between the carbon and the lithiums in **4** which would give rise to a multiplet structure with unresolved ¹³C,⁶-Li couplings.

In order to obtain additional structural information about **4**, as for instance the aggregation state, we performed the ¹H,¹H-NOESY and ⁶Li,¹H-HOESY ex-

(11) Hilmersson, G.; Davidsson, Ö. *Organometallics* **1995**, *14*, 912.

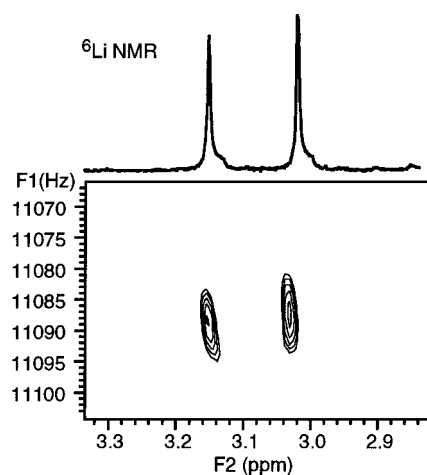
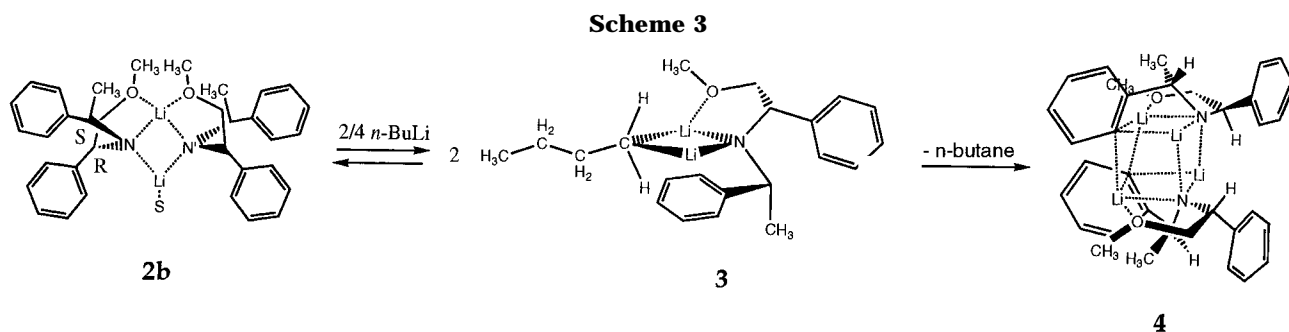


Figure 2. Two-dimensional phase-sensitive ${}^6\text{Li}, {}^6\text{Li}$ -IN-ADEQUATE contour plot of **4** in $\text{DEE-}d_8$ at -90°C .

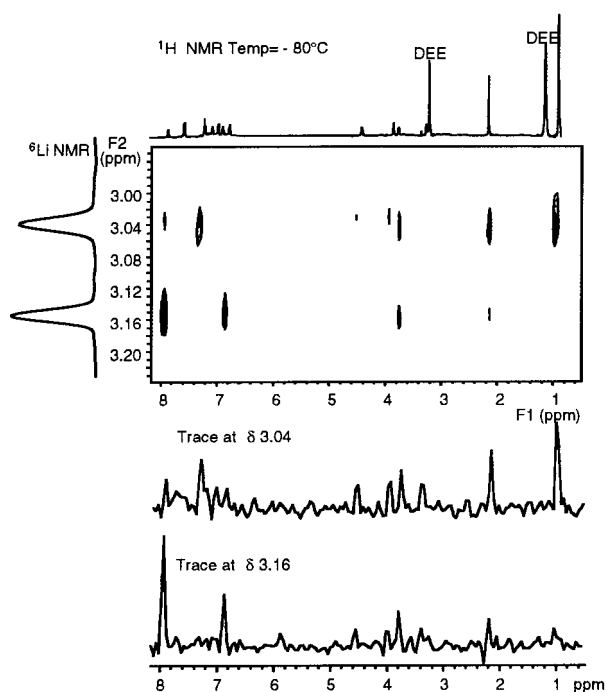


Figure 3. Two-dimensional phase-sensitive ${}^6\text{Li}, {}^1\text{H}$ -HOESY contour plot of **4** in $\text{DEE-}d_8$ at -90°C . The traces at δ 3.08 and 3.19 are also shown.

periments (Figure 3). The correlations found in the ${}^6\text{Li}, {}^1\text{H}$ -HOESY experiment are summarized in Table 3.

The major differences between the two traces at δ 3.04 and 3.16 are seen for the correlations between protons and the lithiums for the methoxy protons, methyl protons, and two phenyl protons adjacent to the lithiated phenyl carbon. For instance, the lithium signal at δ 3.04 shows strong correlations with the CH_3 and OCH_3

protons, indicating that this lithium signal originates from a lithium coordinating one carbanionic carbon atom and two amide nitrogens. These lithiums must on average be more coordinated by the methoxy oxygen atom than the other lithium atoms in the complex. Consequently the lithium signal at δ 3.16 which shows strong NOE's to the phenyl protons originates from a lithium coordinating two carbanionic carbon atoms (phenyl carbons) and one amide nitrogen atom. The methoxy protons in the ${}^1\text{H}$ NMR have a rather unusual large upfield chemical shift of δ 2.18, which must be due to shielding anisotropy effects induced by the close proximity of the methoxy protons to the center of the phenyl rings.

A titration study of **4** in $\text{DEE-}d_{10}$ with $\text{THF-}d_8$ at -80°C was performed. At least six different ${}^6\text{Li}$ NMR signals were observed when 0.26 equiv of THF/Li was reached (Figure 4).

In addition to the two original peaks at δ 3.04 and 3.16 from **4** solvated with DEE, there appeared four additional peaks at δ 2.96, 3.02, 3.18, and 3.35. These new signals are due to a species that is solvated by one THF and one DEE solvent molecule in addition to the two internally coordinating methoxy groups. The large downfield shift observed for one of the new lithium signals, at δ 3.35, is due to the fact that this lithium cation is solvated by one THF molecule. The coordination of one THF and one DEE solvent molecule seems to perturb the chemical shifts even for the methoxy-coordinated lithium cations and thereby resulting in different chemical shifts for these lithiums. Addition of THF up to 1 equiv of THF/Li gave only two signals at δ 3.35 and 2.96 due to a THF-solvated dimer of **4**. The appearance and disappearance of ${}^6\text{Li}$ NMR signals upon increasing the THF concentration is best explained by, first, a slow ligand exchange rate between free and coordinated THF molecules and second, **4** has to be a dimer with a tetrameric lithium core wherein the four lithiums coordinate either with one solvent molecule or with one methoxy group. Each lithium in the dimer **4** is tetracoordinated. This titration study also shows that THF expels DEE. The ${}^6\text{Li}$ NMR signals broadened and disappeared upon addition of THF above 10 equiv of THF/Li , possibly due to formation of polymorphous species and not monomers. The ${}^6\text{Li}$ NMR signals could not be retained at any temperature (20 to -90°C). However, **1** was retained after addition of H_2O without any signs of racemization or other modification.

By comparing ${}^6\text{Li}$ T_1 relaxation times of different lithium complexes of **1** and its lithiated analogue, we have obtained further support that **4** is a dimer. Interestingly, larger aggregates have longer T_1 times, which might be a consequence of higher symmetry in

Table 3. Proton-Proton and Proton-Lithium NOE's in 4^a

proton no.	δ_{H}	H,H-NOE's	H,Li-NOE's to lithium at δ 3.04	H,Li-NOE's to lithium at δ 3.16
2	3.80	OCH ₃ ; 9a(s); 13(w); 4(w); 8(w); 15(w)	X	X
4, 8	7.62	OCH ₃ ; CH ₃ ; 5; 7; 9a; 9b(s); 2(w); 10(w)	X	
5, 7	7.31	OCH ₃ ; CH ₃ ; 4; 6; 8; 9b(w); 9a(w)	X	
6	7.16	5; 7; 9b(w)		
9a	3.35	OCH ₃ ; 2(s); 9b; 4; 8	X	X(w)
9b	3.98	10(s); 4(s); 8(s); 5(w); 6(w); 7(w); 13(w); 14(w)	X	X(w)
10	4.54	OCH ₃ ; 9b(s); 12(s); 4(w); 5(w); 7(w); 8(w); 15(w)	X	X(w)
12	7.05	CH ₃ ; OCH ₃ (w); 10(s)	X	
13	7.17			
14	6.86	OCH ₃ ; CH ₃ ; 15(s); 9b	X	X(s)
15	7.91	OCH ₃ ; CH ₃ ; 14(s); 2; 10(w)	X	X(s)
CH ₃	0.98	10; 5(w); 7(w); 9b(w)	X(s)	
OCH ₃	2.18	CH ₃ ; 2; 4; 8; 9a; 14; 15; 5(w); 7(w); 12(w); 13(w)	X(s)	X

^a Abbreviations: s, strong NOE's; w, weak NOE's.

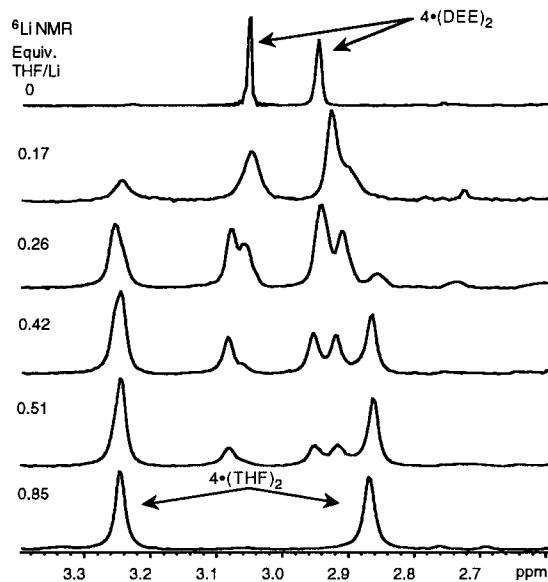


Figure 4. ⁶Li NMR spectra of **4** at different equivalents of THF added in DEE-*d*₈ at -80 °C.

these complexes compared to the unsymmetric but smaller dimers. Furthermore, shorter T_1 times are observed for tricoordinated lithiums compared to tetra-coordinated ones. Both aggregation states and lithium coordination number have been determined by NMR for several lithium amides. Consequently these T_1 measurements could be used as references for the determination of aggregation state and solvation number of analogous lithium amides (Table 4).

Results obtained from ¹H,¹H-NOESY, ¹H,⁶Li-HOESY, ⁶Li,⁶Li-INADEQUATE, ⁶Li NMR temperature dependence, titration study of **4** and T_1 measurements showed that **4** forms a dimer with a tetrameric lithium core where each lithium coordinates with one solvent molecule or one methoxy oxygen. From these NMR studies we have been able to propose a reasonable solution structure for the dimer of **4**, in diethyl ether at -80 °C. Despite fast intramolecular lithium exchange in **4**, we believe that the solution structure of **4** is mostly maintained at higher temperatures, based upon the observation that there is no observable temperature dependence of the ¹H NMR or ¹³C NMR chemical shifts of **4** in the temperature range from 20 to -100 °C. Only temperature dependent line shape changes associated with slow rotation of a phenyl ring are observed around -80 to -100 °C in the ¹H NMR spectrum.

Table 4. T_1 Relaxation Times of Different Chiral Lithium Amide Complexes in Various Solvents at -80 °C

complex	Li-X core	T_1 relaxation times (s)
2 /THF	dimeric	2.2 ^a and 5.4
2 /DEE	dimeric	1.8 ^a and 4.9
2 /cyclohexene oxide	dimeric	2.1 ^a and 5.9
3 /DEE ^b	dimeric	2.5 and 7.0
3 /THF	dimeric	3.4 and 4.9
5 /THF	dimeric	1.9 ^a and 4.8
5 /DEE	dimeric	3.3 ^c
4 /DEE	tetrameric	11.0 and 10.0
(<i>n</i> -BuLi) ₄ /DEE	tetrameric	8.0
2 /THF	monomeric	5.0
2 /TMEDA	monomeric	3.7
2 /cyclohexene oxide	monomeric	4.6

^a Three-coordinated lithium. ^b Dimer determined from observed ⁶Li,¹³C-couplings. ^c Symmetrical dimer.

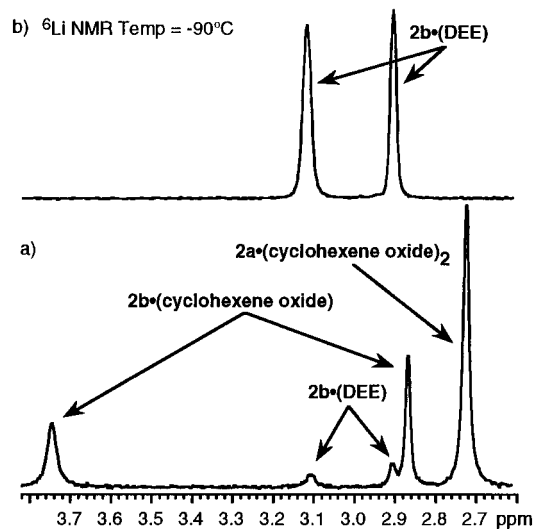


Figure 5. ⁶Li NMR spectra of **2** in DEE-*d*₈ (a) with and (b) without added cyclohexene oxide at -90 °C.

Lithium Amide-Cyclohexene Oxide Complex. The ⁶Li NMR spectrum of **2b** in DEE at -78 °C changed upon addition of cyclohexene oxide. The two lithium signals from **2b** at δ 2.90 and 3.10 decreased in intensity, and three new lithium signals appeared at δ 2.72, 2.86, and 3.74 (Figure 5). The ⁶Li,¹H-HOESY and ⁶Li,⁶Li-EXSY spectra and a temperature dependent ⁶Li NMR study of **2b** and cyclohexene oxide revealed that these three new ⁶Li NMR signals were due to the formation of two different cyclohexene oxide-lithium amide complexes.

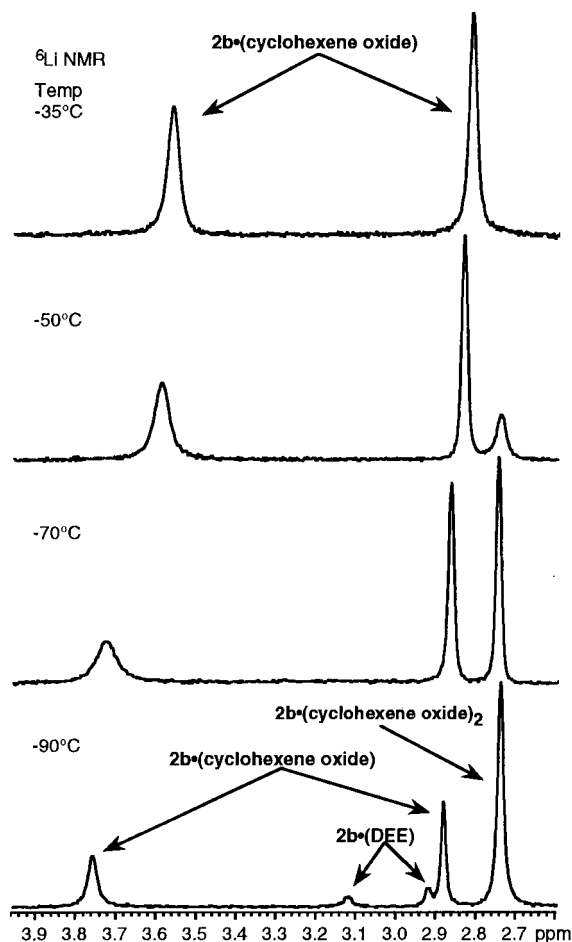


Figure 6. ^6Li NMR spectra of **2** in $\text{DEE-}d_8$ with 2 equiv of cyclohexene oxide/Li added at different temperatures.

First, DEE complexed **2b** in very small amount with two lithium signals at δ 2.90 and 3.10. Second, one set of lithium signals at δ 2.86 and 3.74 from cyclohexene oxide complexed **2b**. Finally, one lithium signal at δ 2.72 from the cyclohexene oxide complexed **2a**. The lithium signal at δ 2.72 increased upon lowering the temperature to -80°C at the expense of the intensity of the lithium signals at δ 2.86 and 3.74. At -35°C there were only two signals observed at δ 2.86 and 3.74 for **2b**-cyclohexene oxide (Figure 6).

Thus this temperature study shows the presence of a monomer/dimer equilibrium. Due to entropy reasons the smaller and more solvated aggregate dominates at low temperature. The ^6Li , ^6Li -EXSY shows that there is a DEE/cyclohexene oxide ligand exchange between the two three-coordinated lithiums appearing at δ 3.10 and 3.74. An exchange is also observed between cyclohexene oxide complexed **2a** and **2b** (Figure 7). The ^6Li , ^1H HOESY showed correlations between the lithium signal at δ 2.72 and cyclohexene oxide protons at δ 1.75, 1.92, and 3.04 (Figure 8).

Weak correlations were observed between the lithium signal at δ 3.74 and cyclohexene oxide protons, and there was no detectable correlation between the lithium signal at δ 2.86 and cyclohexene oxide. The lithium-cyclohexene oxide correlations obtained for the complex **2a**-(cyclohexene oxide) n were strong compared to these obtained between cyclohexene oxide and the lithium signals at δ 2.86 and 3.74 respectively from the **2b**-cyclohexene oxide complex. This difference in correlation intensities between the complexes **2a**-(cyclohexene

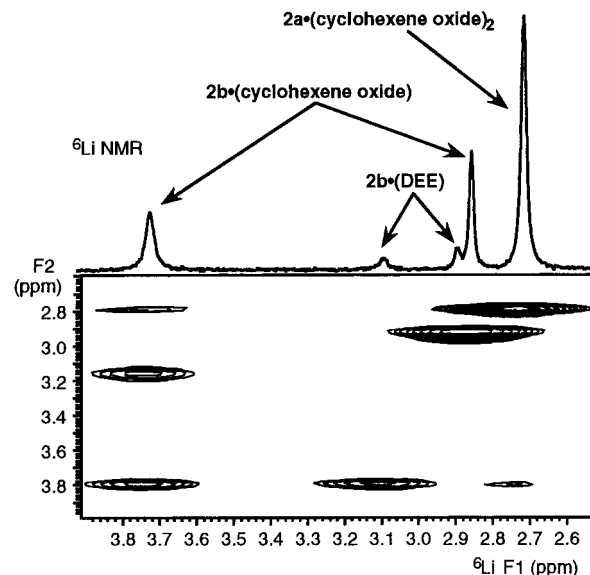


Figure 7. Two-dimensional nonsymmetrized phase-sensitive ^6Li , ^6Li -EXSY contour plot of **2** in $\text{DEE-}d_8$ at -90°C with 2 equiv of cyclohexene oxide/Li added.

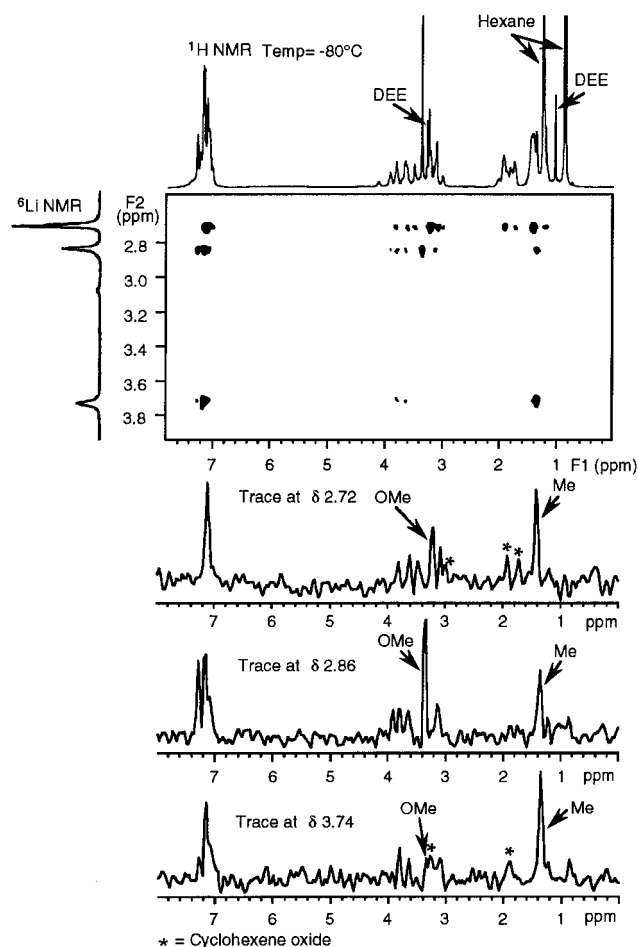


Figure 8. Two-dimensional phase-sensitive ^6Li , ^1H -HOESY contour plot of **2** in $\text{DEE-}d_8$ at -90°C with 2 equiv of cyclohexene oxide/Li added. The ^6Li , ^1H -HOESY traces at δ 2.72, 2.86, and 3.74 are also shown.

oxide) n and **2b**-cyclohexene oxide could be interpreted in such a way that there are two molecules of cyclohexene oxide coordinating to **2a**, i.e. **2a**-(cyclohexene oxide) 2 compared to one in **2b**-cyclohexene oxide.

These observations of initial state structures show that the transition state might be dimeric or monomeric.

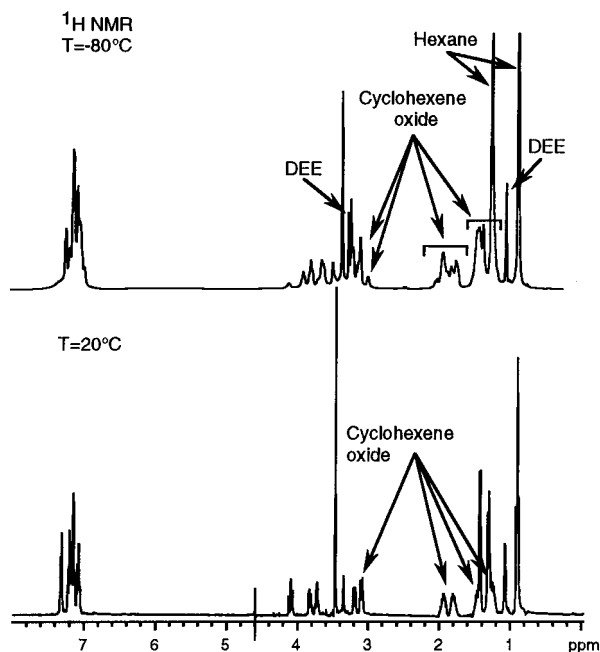


Figure 9. ^1H NMR spectra of **2** in $\text{DEE-}d_8$ with 2 equiv of cyclohexene oxide/Li added at different temperatures.

One has to be very careful in the interpretation of these heteronuclear NOE's as they only show an average initial state structure in solution that did not necessarily lead to a similar transition state structure. However, the increase of the acidity of a C–H bond, for instance in the complexed cyclohexene oxide, due to lithium–proton agostic interactions makes us believe that both the monomer and the dimer complexes could be the reacting species and thereby responsible for the induction of asymmetry in the deprotonation reaction.

Agostic interactions have previously been invoked to explain directing effects of coordinating functional groups. Furthermore, a consequence of agostic interactions between lithium and protons is an increase of the acidity of the C–H bond.^{12,13} The agostic interaction concept both in HOESY NMR and in MNDO calculations has been showed to be of great importance concerning organolithium chemistry. However, agostic activation observed for ortho-directing groups is generally observed in calculations with semiempirical methods (MNDO, PM3), but this is not the case when high-level ab initio calculations are used. Furthermore, the observed agostic interactions might also be an artifact of the method caused by an overestimation of the RLi–HR interaction.

There is no allylic alcohol formed if the temperature is maintained below 0 °C; this is also clearly seen in the ^1H NMR spectrum of **3** and cyclohexene oxide in DEE (allylic proton resonances appear normally at around δ 5.5) (Figure 9). In the ^{13}C NMR spectrum of

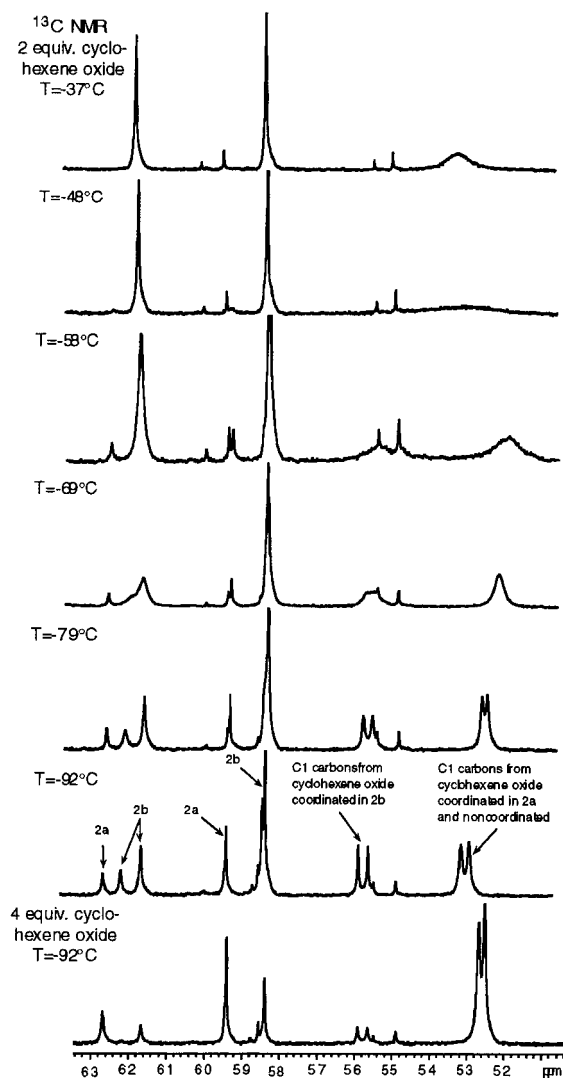


Figure 10. ^{13}C NMR spectra of **2** in $\text{DEE-}d_8$ with 2 equiv of cyclohexene oxide/Li added at different temperatures and a ^{13}C NMR spectrum at -95 °C with 4 equiv of cyclohexene oxide/Li.

2b and the prochiral cyclohexene oxide in DEE at ambient temperature, we observed the formation of a non-isochronous complex. Two nonequivalent sets of ^{13}C NMR signals, at δ 53.57 and 53.85, were observed from the C_α carbons of cyclohexene oxide complexed with **2b**.

A maximum chemical shift separation of approximately 27 Hz was obtained at about 1 equiv of cyclohexene oxide/Li. However, upon addition of cyclohexene oxide above 4 equiv/Li we observed a decrease down to 15 Hz in the chemical shift separation between these two sets of ^{13}C NMR signals. The lithium amide **2** thus functions in the same manner as a chiral solvating agent where the largest chemical shift separation is obtained at a 1:1 ratio.

Upon the temperature signal being lowered, broadening and coalescence were observed at -20 °C for the two nonequivalent ^{13}C NMR signals. However, at -80 °C the nonequivalence of the ^{13}C NMR signals reappeared and four new ^{13}C NMR signals for the C_α carbons of cyclohexene oxide complexed with **2b** and **2a** were observed at δ 55.93, 55.69 and δ 52.38, 52.27, respectively, (Figure 10).

(12) Brookhart, M.; Green, M. L. *J. Organomet. Chem.* **1983**, *250*, 395. Brookhart, M.; Green, M. L.; Wang, L. L. *Prog. Inorg. Chem.* **1988**, *36*, 1.

(13) Bauer, W.; Clark, T.; Schleyer, P. v. R. *J. Am. Chem. Soc.* **1987**, *109*, 970. Bauer, W.; Feigel, M.; Muller, G.; Schleyer, P. v. R. *J. Am. Chem. Soc.* **1988**, *110*, 6033. Kaufmann, E.; Raghavachari, K.; Reed, A. E.; Schleyer, P. v. R. *Organometallics* **1988**, *7*, 1597. Bauer, W.; Schleyer, P. v. R. *J. Am. Chem. Soc.* **1989**, *111*, 7191. Suner, G. A.; Deya, P. M.; Saa, J. M. *J. Am. Chem. Soc.* **1990**, *112*, 1467. Saa, J. M.; Deya, P. M.; Suner, G. A.; Frontera, A. *J. Am. Chem. Soc.* **1992**, *114*, 9093. Saa, J. M.; Morey, J.; Frontera, A.; Deya, P. M. *J. Am. Chem. Soc.* **1995**, *117*, 1105.

The two ^{13}C NMR signals at δ 55.93 and 55.69 from the C α carbons of cyclohexene oxide are due to the formation of non-isochronous complexes with **2b**. The separation was found to be 33 Hz at -80°C , and it was unaffected by increased additions of cyclohexene oxide. The two ^{13}C NMR signals at δ 52.38 and 52.27 with a chemical shift separation of 27 Hz was found to merge upon increased cyclohexene oxide concentration. Furthermore, the ^{13}C NMR chemical shift of these latter signals showed a downfield drift with decreasing temperature and an upfield shift with increasing cyclohexene oxide concentration. This could be explained by the fact that there is a fast ligand substitution rate on the NMR time scale between lithium amide-complexed and noncomplexed cyclohexene oxide. The addition of cyclohexene oxide affects the chemical shift and the chemical shift separation between the two signals at δ 52.38 and 52.27 at -80°C ; thus there is a fast ligand exchange rate in **2a** complexing cyclohexene oxide. The insensitivity of the chemical shift and the chemical shift separation between the ^{13}C NMR signals at δ 55.93 and 55.69 upon temperature and cyclohexene oxide concentration show that there is a slow ligand substitution rate of cyclohexene oxide coordinating **2b**. The drift of the ^{13}C NMR signals from noncoordinated and coordinated cyclohexene oxide in **2a** with temperature could be explained by the fact that the coordination number in the monomer increases and the weighted average chemical shift for noncoordinated and coordinated cyclohexene oxide in **2a** will be shifted more toward the chemical shift for cyclohexene oxide coordinated in **2a**. Furthermore, the large upfield chemical shift upon increased additions of cyclohexene oxide is explained by the fact that the amount of noncoordinated cyclohexene oxide increases and thereby the weighted average chemical shift will be shifted more toward the chemical shift for noncoordinated cyclohexene oxide. Observations of slow ligand substitution rates in organolithium compounds have previously been reported.¹⁴ The lack in observing slow ligand substitution rates in **2a** tell us that there has to be at least two cyclohexene oxide molecules coordinating in **2a**; previous studies of substitution rates of THF solvated **2** have shown that there are two THF molecules coordinating in **2a**.

A titration study of **4** in DEE with cyclohexene oxide at -80°C was performed, and at 0.5 equiv of cyclohexene oxide/Li, four lithium-6 signals were observed. The two lithium-6 signals at δ 3.67 and 2.91 are due to the formation of a coordination complex between one cyclohexene oxide one DEE molecule and **4**, and the two lithium-6 signals at δ 3.04 and 3.16 are due to a complex between two molecules of DEE and **4**. Further addition of cyclohexene oxide up to 4 equiv/Li gave a lithium-6 NMR spectrum consisting of only two signals at δ 3.42 and 2.92 from a solvation complex between two cyclohexene oxide molecules and **4**.

The ^{13}C NMR showed the presence of slow ligand substitution rates on the NMR time scale at 0.5 equiv of cyclohexene oxide/Li as two separate signals was observed from cyclohexene oxide. Two ^{13}C NMR signals centered at δ 55.5 were obtained from coordinated

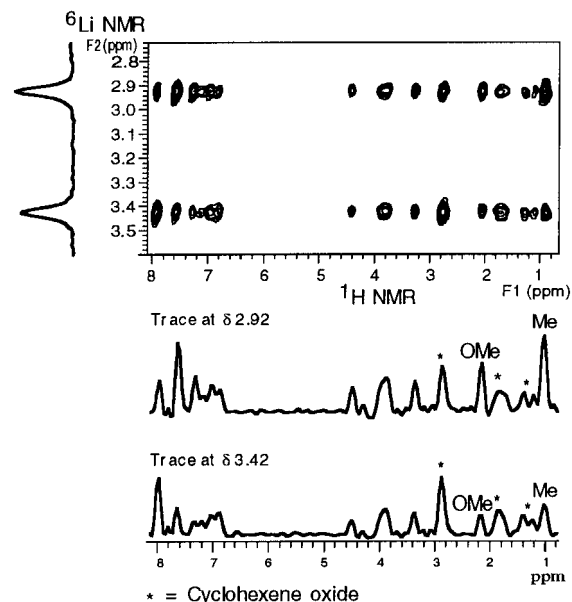


Figure 11. Two-dimensional phase-sensitive $^6\text{Li},^1\text{H}$ -HOESY contour plot of **4** in $\text{DEE}-d_8$ with 2 equiv of cyclohexene oxide/Li added at -85°C . The $^6\text{Li},^1\text{H}$ -HOESY traces at δ 2.92 and 3.42 are also shown.

cyclohexene oxide. The splitting pattern is due to reasons previously discussed for cyclohexene oxide coordinating to **2b**. At δ 55.0 a broad signal was observed with no visible splitting. This signal increased upon further addition of cyclohexene oxide. Therefore, we assign this signal to noncoordinated cyclohexene oxide. As the amount of cyclohexene oxide was increased to 4 equiv/Li, we observed a line broadening of the ^{13}C NMR signals from both cyclohexene oxide and **4**. This increase in line broadening of the ^{13}C NMR signals has to be due to an increase in the ligand substitution rate. Even if the temperature was lowered to -110°C , we were not able to obtain two sharp ^{13}C NMR signals from the coordinated cyclohexene oxide as observed at 0.5 equiv of cyclohexene oxide/Li. The effect that the ligand substitution rate increased with an increased amount of cyclohexene oxide shows that there is an associative mechanism that controls the ligand substitution. Furthermore, three sets of ^{13}C NMR signals were also observed from **4**, one from DEE, one from cyclohexene oxide/DEE, and one from cyclohexene oxide solvated **4**, due to this slow ligand substitution rates. Further addition of cyclohexene oxide above 1 equiv/Li resulted in the disappearance of these sets of ^{13}C NMR signals.

The $^1\text{H},^6\text{Li}$ -HOESY spectrum showed strong correlations between cyclohexene oxide and the two lithium signals from **4** as expected (Figure 11).

Deprotonation of Cyclohexene Oxide. The deprotonation reaction of cyclohexene oxide using **2** and **4** did not proceed at temperatures below 0°C . However, at ambient temperature the reaction proceeded with reaction half-times, yields, and stereoconfiguration as shown below in Table 5 and Scheme 4.

The shorter half time and the inversion of stereoconfiguration in the product using **4** instead of **2** is due to the fact that the deprotonation is not performed by the amide base but rather by the carbanionic base. Furthermore, the solution state structure of **4** is also quite different from **2**. In addition it was observed that the

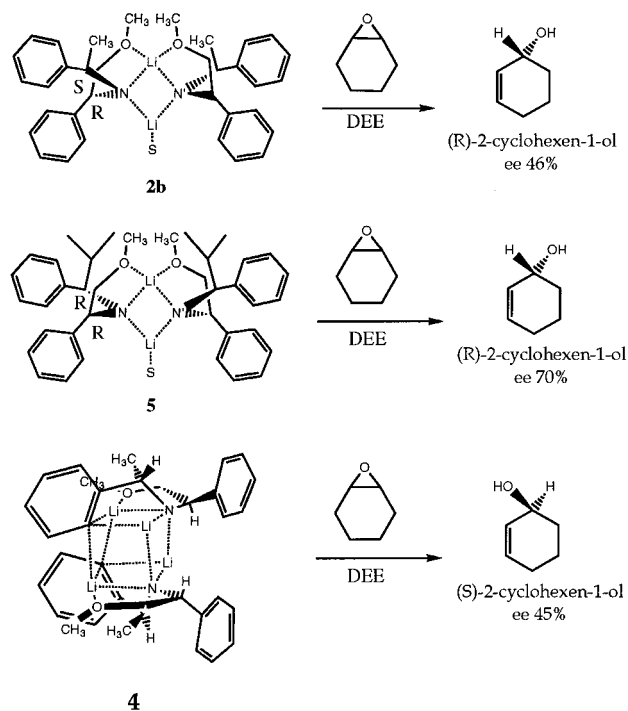
(14) Lucht, B. L.; Collum, D. B. *J. Am. Chem. Soc.* **1994**, *116*, 6009. Reich, H. J.; Green, D. P. *J. Am. Chem. Soc.* **1989**, *111*, 8729. Lucht, B. L.; Collum, D. B. *J. Am. Chem. Soc.* **1994**, *117*, 9863. Hilmersson, G.; Davidsson, Ö. *J. Org. Chem.* **1995**, *60*, 7660. Lucht, B. L.; Collum, D. B. *J. Am. Chem. Soc.* **1996**, *118*, 2217.

Table 5. Results from the Deprotonation of Cyclohexene Oxide Using **2, **4**, and the Lithium Salt of **5** in THF and/or DEE at 20.0 °C**

lithium amide	solvent	half-life (h)	rate constant (min ⁻¹)	e.e (%)	config of cyclohexenol
2	THF	50.7	2.28×10^{-4}	47	<i>R</i>
2	DEE	43.5	2.66×10^{-4}	47	<i>R</i>
4	DEE	33.5	3.45×10^{-4}	41	<i>S</i>
5	THF	17.4	— ^a	74	<i>R</i>
5	DEE	21	— ^a	70	<i>R</i>

^a Not determined.

Scheme 4



enantiomeric excess was at its peak at an early stage of the reaction and decreasing thereafter when **4** was used. This means that **4** reacts fast with cyclohexene oxide, forming **2** and (*S*)-cyclohexen-1-ol. The formed lithium amide **2** then reacts with cyclohexene oxide but with reversed enantioselectivity in the product ((*R*)-cyclohexen-1-ol) and thus the total ee decreases.¹⁵ Our NMR and X-ray studies of **2** in DEE, THF, and cyclohexene oxide suggested that a more sterically demanding substituent than a methyl group at the C(10), C(27) carbons in **2** would enhance the selectivity, this if a dimer was considered as the reacting species in the transition state. A semiempirical (PM3) calculation was performed starting from the determined X-ray geometry of **2**·THF. The ligand at the three-coordinated lithium in the above X-ray structure was exchanged from a THF to a cyclohexene oxide in the PM3 calculations, reached a minimum, as confirmed by frequency calculation (Figure 12).

The isopropylamine analogue **5** was prepared to test the hypothesis that it is the bulkiness at the C(10), C(27) carbons that is important for controlling the enantiomeric excess. This suggestion turned out to be a correct

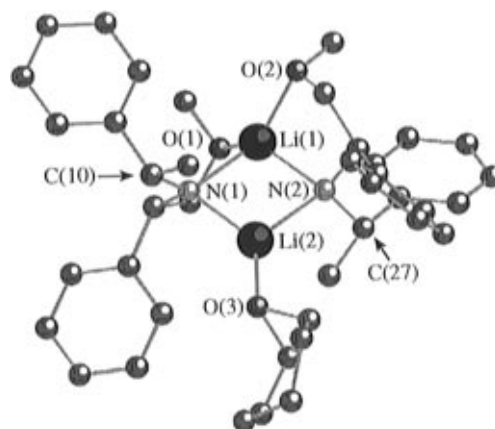


Figure 12. Ball and stick (hydrogens has been omitted for clarity) view of **2** complexing cyclohexene oxide, obtained from a PM3 geometry optimization of the obtained X-ray crystallographic geometry of **2**·THF, showing the steric interaction between cyclohexene oxide and the methyl groups at the C(10), C(27) carbons.

conclusion, as a far better selectivity in the deprotonation reaction was obtained, the ee increased from 47% to 74% with the same stereoconfiguration in the product. The ⁶Li NMR of the lithium salt of **5** in DEE at -85 °C gave one major lithium signal at δ 1.32 and a minor one at δ 1.88. The T_1 for the signal at δ 1.32 was 3.3 s, which supports the idea that this signal originates from a symmetrical dimer (Table 2). (The lithium salt of **5** in toluene also gave one major peak in the ⁶Li NMR spectrum at δ 1.35.) The addition of THF to the above solution resulted in the appearance of two new lithium signals at δ 2.40 and 1.94 with T_1 of 4.8 and 1.9 s, respectively. The ⁶Li, ¹H-HOESY revealed correlations between the THF ¹H NMR signals at δ 1.40 and 3.60 and the lithium signal at δ 1.94, respectively. Correlations were also observed between the THF ¹H NMR signals at δ 1.53, 3.40 and the lithium signal at δ 2.40, respectively. This lithium signal δ 2.40 also showed very strong correlations to the methoxy group protons at δ 2.80, which was not observed for the lithium signal at δ 1.94. These results shows that these two new lithium signals at δ 2.40 and 1.94 are due to a THF-solvated dimer of the lithium salt of **5** wherein the lithium signal appearing at δ 1.94 originates from a three-coordinated lithium (coordinating to two amide nitrogen atoms and one THF oxygen atom) and the lithium signal appearing at δ 2.40 originates from a lithium that is tetracoordinated (coordinating two amide nitrogen atoms and two methoxy oxygen atoms). The lithium salt of **5** gives as its analogue **2** an unsymmetrical dimer when solvents/ligands with good coordinating ability to lithium is used, as for instance THF. We were not able to observe any slow ligand substitution rates on the NMR time scale for the lithium salt of **5** coordinating THF. The crystal structure of compound **6**, which is the hydrochloric salt of **5**, was determined by X-ray crystallography (see Figure 13 and Table 1) and the configuration showed to be *R,R*. Although an absolute configuration determination is not necessary in this case since one center was known to be *R*, the crystallographic absolute structure parameter also clearly favors *R,R* over *S,S*. The unit cell comprises two crystallographically independent molecules, and a polymeric structure is formed via hydrogen-bonded N \cdots Cl contacts around 3.2 Å.

(15) The absolute configuration was determined by the comparison of the chromatogram from a deprotonation reaction of cyclohexene oxide using a chiral lithium amide described by Asami and co-workers, which has been reported to give the (*S*)-cyclohexen-1-ol in an ee of 80%.^{3b-d}

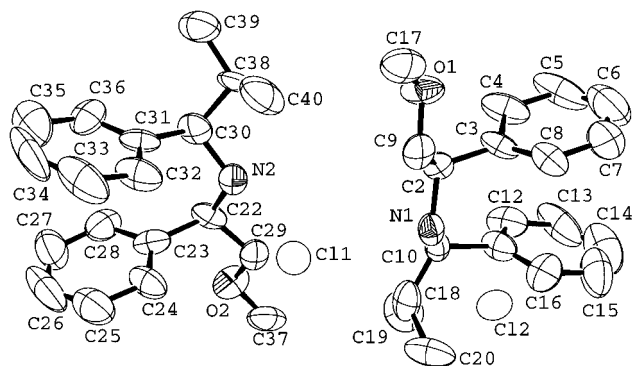


Figure 13. Crystallographic numbering in (*R,R*)-**6**. The two crystallographically independent molecules are stereochemically equivalent.

Despite this, the deprotonation–ring opening of cyclohexene oxide gave the same stereoconfiguration in the product, namely the (*R*)-cyclohexen-1-ol. This increase in ee could be explained since instead of the sterically demanding isopropyl substituent interacting with the cyclohexene oxide as proposed, there will now be a phenyl group at this position. The bulkiness of the isopropyl (*A* value 2.1) is almost the same as for the phenyl group (*A* value 2.9).

This result shows the large potential in studying initial states, for the improvement and understanding of factors controlling asymmetric reactions. However, as stated before, none of the results presented here exclude the possibility of a monomeric transition state.

Experimental Section

General. Glassware was dried overnight in a 120 °C oven (syringes and Teflon containing parts were dried at 50 °C in a vacuum oven) prior to transfer into a glovebox (Mecaplex GB 80 equipped with a gas purification system that removes oxygen and moisture) with a positive nitrogen atmosphere. The typical content of moisture was less than 0.5 ppm in the atmosphere. All manipulations of the lithium compounds were carried out in the glovebox using gastight syringes. The preparation of *n*-butyllithium was carried out under a positive pressure of argon.

All solvents used were dried according to literature procedure, prior to storage over Deporex Fluka molecular sieves and stored in the glovebox. All NMR tubes were sealed by the Wilmad/Omnifit OFV Teflon valve system with Teflon/silicone septa.

(2-Methoxy-(*R*)-1-phenylethyl)((*S*)-1-phenylethyl)amine (1). This amine was synthesized according to literature methods.⁷

[⁶Li]Lithium (2-Methoxy-(*R*)-1-phenylethyl)((*S*)-1-phenylethyl)amide (2). This amide was generated in situ in the NMR tube by the addition of 35 μL (0.35 mmol) of 10 M [⁶Li]-*n*-butyllithium to a solution of (2-methoxy-(*R*)-1-phenylethyl)-((*S*)-1-phenylethyl)amine (90 mg, 0.35 mmol) in 0.7 mL of DEE-*d*₁₀ at –60 °C.

Single crystals suitable for X-ray studies was prepared as follows. **1** (100 μL, 0.35 mmol) was dissolved in 1 mL of dry toluene in a Schlenk tube, and to this solution was added 30 μL (0.37 mmol) of 10 M *n*-BuLi at –70 °C. To the above solution was added 1 equiv of THF/Li, 52 μL (THF assumed to be 14M). From this solution single crystals precipitated after 1 week at –20 °C.

[⁶Li]Lithium (2-Methoxy-(*R*)-1-phenylethyl)(2-(⁶Li)thio)-(S)-1-phenylethyl)amide (4). To a [⁶Li]lithium-(2-methoxy-(*R*)-1-phenylethyl)-((*S*)-1-phenylethyl)amide DEE-*d*₁₀ solution obtained as described above was added 1 additional equiv of 10 M [⁶Li]-*n*-butyllithium (35 μL, 0.35 mmol). The

reaction mixture was allowed to equilibrate at 25 °C in the NMR magnet. The reaction was completed after approximately 5 h. The reaction was monitored by ¹H NMR by observation of the decrease of the Ha from *n*-BuLi at δ –1.1 and the increase of the methoxy signal at δ 2.18 of **4**.

(*R*)-(-)-1-(Aminophenyl)-2-methoxyethane was prepared by a method similar to one reported by Meyers et al.¹⁶ (*R*)-Phenylglycinol (10.1 g, 73.6 mmol) in dry THF (100 mL) was added dropwise over 2 h to a slurry of sodium hydride (1.85 g, 77.3 mmol) in 50 mL of dry THF under a nitrogen atmosphere. The resulting gelatinous pale green-yellow solution was kept at room temperature overnight. Methyl iodide (4.58 mL, 73.6 mmol) in dry THF (50 mL) was added dropwise over 2 h. The reaction was maintained at room temperature for 3 h and then at slightly elevated temperature (40 °C) for another hour. Meanwhile mixing was accomplished by means of an overhead stirrer. The resulting nonviscous orange solution was poured into a cooled saturated sodium chloride solution and extracted with DEE (4 × 150 mL). The combined ether layers were washed with brine, dried over Na₂SO₄, and concentrated to yield 11.42 g of crude product. Distillation (bp 60 °C; 1.7 mbar) gave a clear oil. Yield: 10.1 g; 91%. The flask was flushed with nitrogen, stoppered, and kept in a refrigerator for months. Analysis by NMR, GC–MS (CI ionization), and IR spectroscopy showed no sign of N-methylation.

***N*-(*R*)-2-Methoxy-1-Phenyl-(*R*)-α-isopropylbenzylamide (5).** A solution of (*R*)-(-)-1-(aminophenyl)-2-methoxyethane (8.0 g, 52.95 mmol), isobutyrophenone (7.85 g, 53.0 mmol), and a catalytic amount of *p*-toluenesulfonic acid in benzene (100 mL) was refluxed for 90 h under continuous removal of water by means of a Dean–Stark trap. After cooling, the reaction mixture was washed with aqueous Na₂CO₃ (100 mL) and saturated NaCl (100 mL), dried over MgSO₄, and concentrated to yield 18.8 g of a yellowish oil.

This resulting oil was dissolved in 150 mL of dry THF and catalytically hydrogenated using Pd/C (10%) in a Parr apparatus at 4 atm (H₂) overnight without further purification. The mixture was filtered and concentrated to give 18.3 g of a very pale yellow oil. Distillation gave a fraction boiling at 120 °C (<1 mbar) that was found to contain a mixture of the *R,R* and *R,S* diastereomers in a 2:1 ratio. Yield: 9.21 g; 61% yield.

***N*-(*R*)-2-Methoxy-1-phenyl-(*R*)-α-isopropylbenzylamide Hydrochloride (6).** Treating the diastereomeric mixture of **5** with HCl (100 mL, 1 M), washing with DEE, and evaporating the aqueous acid solution afforded **6**. Repeated recrystallization of **6** gave exclusively the *R,R* diastereomer as established by X-ray diffraction. Liberation of the free amine was afforded by treating **6** with cool NaOH and extracting the free amine into ether, drying, and evaporating the solvent. Yield: 25%. [α]_D²⁰ = –11.8° (*c* = 3.0; EtOH). ¹H NMR (δ, ppm): 0.75 (3H, d, *J*₁₂ 6.7, CH₃); 0.96 (3H, d, *J*₁₂ 6.7 CH₃); 1.11 (1H, t, *J*₁₂ 6.7); 1.87 (1H, 8 signals, *J*₁₂ 6.5); 2.17 (1H, br, N-H); 3.26 (3H, s, OCH₃); 3.33 (1H, br); 3.37 (1H, dd, *J*₁₂ 7.0); 3.41 (2H, dd, *J*₁₂ 5.4, 7.0); 3.82 (1H, dd, *J*₁₂ 5.4); 7.01–7.14 (m, 10H, aromatic protons). ¹³C NMR (δ, ppm): 19.6 (q, CH₃); 20.0 (q, CH₃); 35.1 (d); 58.9; (q, OCH₃) 62.1 (d); 68.8 (d); 77.9 (t); aromatic carbons 126.9, 127.3, 128.1, 128.3, 128.8; quaternary carbons 143.2, 144.4.

Titration Studies by Cyclohexene Oxide. To the DEE-*d*₁₀ solution of **2** or **4** were added small amounts of cyclohexene oxide at –80 °C with a gas-tight syringe, and the ⁶Li, ¹H, and ¹³C NMR spectra were recorded at this temperature after each addition of cyclohexene oxide. There was no trace of deprotonation product visible in the ¹H NMR if the temperature was held below 0 °C.

Titration Studies of 4 by THF. To the DEE-*d*₁₀ solution of **4** was added small amounts of THF at –80 °C with a gas-tight syringe, and the ⁶Li, ¹H, and ¹³C NMR spectra were recorded at this temperature after each addition of THF.

(16) Meyers, A. I.; Poindexter, G. S.; Brich Z. *J. Org. Chem.* **1978**, *43*, 892.

General Protocol for Cyclohexene Oxide Deprotonation Experiments. The amine (530 μmol) was dissolved in 2.5 mL of dry THF or DEE. The reaction flask was cooled to 0 °C, and an equimolar amount¹⁷ of *n*-butyllithium was added dropwise with a syringe. The reaction vessel was kept for 15 min at 0 °C before transfer to a thermostated bath holding 20.0 °C followed by addition of cyclohexene oxide (50.5 μL , 500 μmol).

At intervals, 20 μL of the reaction mixture was redrawn and quenched with saturated aqueous ammonium chloride (0.5 mL). This mixture was extracted with 1 mL of DEE and dried (Na_2SO_4). Analysis was performed using a chiral capillary GC column of 25 m coated with octakis(6-*O*-methyl-2,3-di-*O*-pentyl)- γ -cyclodextrin. Helium was used as the carrier gas, the column temperature was 80 °C, a racemic mixture of the two enantiomers were baseline separated by using this chiral column, and the order of elution of the (*R*)- and (*S*)-alcohol was determined by injecting a sample containing (*R*)- and (*S*)-alcohol prepared by a method described by Asami which has been reported to give a large enantiomeric excess of the (*S*)-alcohol.^{3,15} The enantiomeric excess was calculated from the relative areas of the two peaks from the two alcohol enantiomers.

Cyclohexene Oxide Deprotonation Experiments Using [⁶Li]Lithium (2-methoxy-(*R*)-1-phenylethyl)(2-([⁶Li]-lithio)-(S)-1-phenylethyl)amide. (2-Methoxy-(*R*)-1-phenylethyl)(S)-1-phenylethylamine (134 μL , 530 μmol) was dissolved in 2.5 mL of dry DEE. The reaction flask was cooled to 0 °C, and 2 equiv of *n*-butyllithium was added with a syringe.¹⁷ The reaction flask was put in a thermostated bath (20.0 °C), and held there for at least 4 h for the formation of the reagent. Cyclohexene oxide (50.5 μL , 500 μmol) was added and the temperature kept at 20.0 °C. The reaction was followed as previously described above by chiral GC.

X-ray Crystallography: General Details. Crystal and experimental data are summarized in Table 1. Diffracted intensities were measured with a Rigaku AFC6R diffractometer using radiation from a RU200 rotating anode source operated at 9 kW (50 kV; 180 mA). The $\omega/2\phi$ scan mode was employed, and stationary background counts were recorded on each side of the reflection, the ratio of peak counting time vs background counting time being 2:1. The intensities of three reflections monitored regularly after measurement of 150 reflections confirmed crystal stability during data collection. Correction was made for Lorentz, polarization, and absorption effects. The structures were solved by direct methods (SHELXS)¹⁸ and refined using SHELXL.¹⁸ Structural illustrations have been drawn with Ortep-3 for Windows.¹⁹

[⁶Li]Lithium (2-Methoxy-(*R*)-1-phenylethyl)(S)-1-phenylethyl)amide (2). A colorless crystal fragment was isolated, cut, and mounted by the use of low-temperature

(17) (*17*) *n*-Butyllithium (Aldich, 1.6 M solution in hexane) was titrated prior to use using 4-biphenylmethanol as described in the following: Juaristi, E.; Martinez-Richa, A.; Garcia-Rivera, A.; Cruz-Sanchez, J. S. *J. Org. Chem.* **1983**, *48*, 2603.

(18) Sheldrick, G. M. *SHELXS-86 and SHELXL-93*; University of Göttingen, Göttingen, Germany, 1986 and 1993.

(19) Farrugia, L. J. *J. Appl. Crystallogr.*, in press.

techniques²⁰ (under argon at -150 °C) and transferred in Lindemann capillaries under liquid nitrogen to the diffractometer. The structure was refined with full-matrix least-squares calculations on F^2 , including anisotropic thermal parameters for the lithium, carbon, nitrogen, and oxygen atoms with the hydrogen atoms (in calculated positions) riding on the respective carbon. Selected interatomic distances and angles are given in Table 2, and the crystallographic numbering is shown in Figure 1.

***N*-(*R*)-2-Methoxy-1-phenyl-(*R*)- α -isopropylbenzylamide Hydrochloride (6).** Data were measured using a colorless crystal which was cut into a cubic shape. Although the cell dimensions indicate a monoclinic crystal, the best result was obtained using the triclinic system. The structure was refined with full-matrix least-squares calculations on F^2 , including anisotropic thermal parameters for the carbon, nitrogen, oxygen, and chloride atoms with the hydrogen atoms (in calculated positions) riding on the respective carbon. The crystallographic numbering in **6** is shown in Figure 13.

NMR Spectroscopy: 2D NMR Measurements. All 2D spectra were acquired using nonspinning 5 mm samples with deuterium field-frequency locking. Spectra were processed in the phase-sensitive mode with square sine bell weighting both in f_1 and f_2 .

For the ⁶Li,¹H-HOESY spectrum, the following parameters were used: spectral window of 1000 Hz ($f_2 = 6\text{Li}$) and 8000 Hz ($f_1 = 1\text{H}$); 256 increments and 16 scans per increment in t_1 ; mixing time 1.0 s; 28 μs proton 90° decoupler pulse.

For the ⁶Li,⁶Li-EXSY spectrum, the following parameters were used: spectral window of 1000 Hz (f_1 and f_2); 256 increments and 8 scans per increment in t_1 ; mixing time 3.5 s.

For the ⁶Li,⁶Li-INADEQUATE spectrum, the following parameters were used: spectral window of 1000 Hz (f_1 and f_2); 64 increments and 8 scans per increment in t_1 ; $\tau = 1.25$ s. The advantage of using the INADEQUATE experiment instead of absolute value COSY is the elimination of obtaining correlations due to uncautious signal weighting.

Acknowledgment. We are grateful to the Swedish Natural Science Research Council (NFR), Lars Hiertas memorial foundation, Wilhelm and Martina Lundgrens science foundation, and Anna Ahrenbergs foundation, for financial support.

Supporting Information Available: Tables giving experimental, positional, and thermal parameters, as well as full geometric data on compounds **2** and **6**, ⁶Li and ¹H,⁶Li-HOESY NMR spectra of the lithium salt of **5**, and table of Cartesian coordinates for the PM3 calculated geometry of 2-cyclohexene oxide (18 pages). Ordering information is given on any current masthead page.

OM960989R

(20) Håkansson, M. *Inorg. Synth.*, in press.